Supplementary Information:

for

Algorithms to automatically quantify the geometric similarity of anatomical surfaces

by

Doug M. Boyer, Yaron Lipman, Elizabeth St. Clair, Jesus Puente, Biren A. Patel, Thomas A. Funkhouser, Jukka Jernvall, and Ingrid Daubechies

in

Proceedings of the National Academy of Sciences 108(43)

PART I

Original data access:

The original surface scans representing datasets A-C (as obtained after pre-processing – see Supplementary Methods #3), as well as observer-determined landmark coordinates are available from the Data Conservancy Project (arXiv #1110.3649) and also at the following URL:

http://www.wisdom.weizmann.ac.il/~ylipman/CPsurfcomp/

Algorithm code access and details on use:

We used programs written in Matlab to compute numerical values for Conformal Wasserstein Neighborhood distances and Continuous Procrustes distances described in the main text. An exact version of the code for the programs for the most successful of the two distances (at least for the applications we considered), i.e. for the Continuous Procrustes distances (used on datasets A-C in the main text) can be obtained from the Data Conservancy Project (arXiv #1110.3649) as well as at the following URL:

http://www.wisdom.weizmann.ac.il/~ylipman/CPsurfcomp/

The latter site will also provide an updating version of the code as the algorithm is developed through further research by the authors and other collaborators. Users should be aware that the programs have a number of parameters that can be adjusted; exact values of these parameters that gave rise to the results given in our tables are listed together with the code. We also wish to stress that **the parameter values we used are non-optimal**. We used values that seemed reasonable for representing surface geometry. Depending on the larger goal the end-user has for the algorithm (e.g., in our case it was to classify specimens into taxonomic groups based on similarity in tooth geometry) a systematic, machine-learning guided search of the parameter space will likely yield improved results. Alternatively, if the user simply inputs uninformed guesses as parameter values this could lead to poor results.

PART II

Supplementary Methods

1. **Description/justification of sample datasets**
2. **Generating digital models of anatomical structures**
3. **Preprocessing of digital models (noise reduction)**
4. **Description/justification of Observer Determined (OD) landmarks**
5. **Generating Procrustes distances between sets of OD landmarks**
6. **Comparing Procrustes distances based on OD landmarks with distances based on GD correspondences**
7. **Topographic variable dataset for comparison to Procrustes distances in taxonomic and dietary classifications**

Supplementary Tables

Supplementary Table 1. Specimens for lower-molar study, colored coded by diet groups assignments used for classification shown in supplementary table 8
Supplementary Table 2. Specimens for first-metatarsal study
Supplementary Table 3. Specimens for radius study
Supplementary Table 4. Classification success rates and failures, 2nd mandibular molar
Supplementary Table 5. Classification success rates and failures, proximal first metatarsal
Supplementary Table 6. Classification success rates and failures, distal radius
Supplementary Table 7. Comparison of taxonomic and dietary classification success rates for analyses of teeth using topographic variables, and automatically determined Procrustes distances.
Supplementary Table 8. Landmark Propagation Error summary statistics

Supplementary Figures

Supplementary Figure 1. Landmarks for lower-molar study
Supplementary Figure 2A-B. Landmarks for first-metatarsal study
Supplementary Figure 3. Landmarks for radius study
Supplementary Figure 4. Difficult cases: teeth from 3 species of Galago
Supplementary Figure 5. Histograms Illustrating Landmark Propagation

Supplementary Discussion

Successes on particularly dfficult cases
Significance of classification errors in second lower molar dataset
Placement of *Megaladapis*
Significance of errors in first metatarsal dataset
Significnce of errors in radius dataset
Discussion of the error in algorithmic approximation to the continuous Procrustes distance
Discussion of Landmark Propogation

Supplementary Methods

1. Description/justification of sample datasets. As described in Results, we tested our algorithm's ability to identify biologically meaningful correspondences using three independent datasets. The first one (dataset A) consists of second mandibular molars (Supplementary Table 1). Only unworn specimens were chosen, as we are interested in evaluating biologically determined shapes, not environmentally altered shapes. There are 116 specimens. Dependent on the taxonomic scheme employed this sample represents up to four orders, 19 families, 35 genera and over 35 species. The second dataset (dataset B) consists of the proximal end of the first metatarsal (Supplementary Table 2), which forms part of the digit ray of the "big toe." This bone articulates with the entocuneiform, a tarsal bone. This sample is comprised of 61 specimens representing primates in nine families, 13 genera and over 13 species. The third dataset (dataset C) represents the distal end of the radius (Supplementary Table 3), the larger of the two forearm bones, whose articular surface contacts the proximal carpal bones of the wrist. This dataset is smaller with only 45 specimens in all, representing hominoids (humans and apes). Specifically, it includes taxa from a single order (primates), two families, four genera and five species. Catalogue numbers for biological specimens can be found in Supplementary methods section 1.

2. Generating digital models of anatomical structures. Digital models of all specimens were created using micro-CT and medical CT imaging devices. A brief description of how the dental models were created follows; however, for a more detailed description see Boyer (1). Dentitions of interest were molded using PresidentJet Plus light body molding material (polyvinylsiloxane). Specimens were cast using EpoTek 301 with mixed with Dynagrout's gray liquid pigment. Specimen casts are then trimmed to the tooth of interest – second mandibular molars. Individual tooth casts were mounted on disks of either 19mm or 36mm diameter using Elmer's Glue.

Larger teeth were placed on the larger disk diameter. Tooth disks were scanned using at Stony Brook University's Center for Biotechnology using Scanco medical μCT-40 machine with scanner settings of 45-70KeV, 177-114μAmp, integration times of 0.3sec, and resolutions of. 10μm (19mm disks) 18μm (36mm disks).

First metatarsals were scanned using a GE eXplore Locus machine with settings of 80KeV, 450μAmp, and resolutions of 20-45μm (depending upon absolute sizes of specimens scanned) at Ohio University MicroCT facility (Athens, Ohio), and a Scanco medical μCT-75 machine with scanner settings of 70KeV, 114μAmp, integration times of 0.2sec, and resolutions ranging from 25-78μm at Stony brook University's Center for Biotechnology.

For the radius dataset, real bones were scanned using medical grade CT machines including a Siemens Somatom AR machine with settings of 110KeV, 63μAmp, and resolution of 120μm (x-y plane) by 1000μm (slice spacing) at the National Museum of Natural History (Washington DC); a GE Light speed 16 machine with settings of 120KeV, 70μAmp, and resolution of 200μm (x-y plane) by 625μm (slice spacing) at Stony Brook University (Stony Brook, New York); and a Philips Brilliance 16 machine with settings of 120KeV, 95μAmp, and resolution of 200μm (x-y plane) by 400μm (slice spacing) at the Anthropologisches Institut und Museum, Universitat Zurich (Zurich, Switzerland).

CT data was exported in DICOM file format. In some but not all cases DICOM stacks were imported as image sequences into ImageJ, cropped, and saved as series of TIFF files. Either DICOM's or TIFF's were then opened in Amira 5.1 or Aviso 6.0. Surfaces were created by using the threshold selection tool in the Labelfield function of Amira and Aviso. Surfaces were saved

using Stanford Polygonal File (PLY) format.

3. Preprocessing of digital models (noise reduction). In a preprocessing stage surfaces are simplified and smoothed. First, we simplify all the surfaces so as to have roughly the same number of points (5K points). For that end we use a standard method (2). Second, we smooth the surfaces. This is also done with standard methods (3, 4), where we use the combinatorial Laplacian to improve the triangle quality, which is desirable for the conformal flattening stage.

4. Description/justification of Observer Determined (OD) landmarks. To evaluate the biological significance of the feature correspondences implied by our algorithm's optimal conformal maps, we generated three datasets of landmarks. The identification of our tooth landmarks is based on descriptive and theoretical studies published over the course of the last 130 years; they are generally accepted as "homologous," or at least corresponding in a biological and geometrical sense, among the taxa in our dataset (5-10). There is no similar history of study supporting landmark designations on the radius or first metatarsal; our landmark decisions were based primarily on knowledge of anatomical orientation and muscle attachments of these bones, recognizable due to the similar geometries exhibited by these features as well as previous studies and descriptions (11, 12). Our conventional landmark dataset was assembled following standard procedures in geometric morphometrics (13). We used the program Landmark Editor (14) to select hypothetically homologous landmarks on digital models. Specifically, for the tooth dataset we placed 18 homologous landmarks on each of these digital models (Supplementary Figure 1), for the first metatarsal dataset two different researchers placed independently chosen sets of 11 landmarks on each model (Supplementary Figure 2a-b), and for the radius dataset we placed 13 landmarks on each model by one observer (Supplementary Figure 3). E. St.Clair identified and placed OD landmarks of dataset A. D. M. Boyer (observer 1) defined and placed one set of OD landmarks for dataset B, while E. St. Clair (observer 2) defined and placed another. For dataset C, B. A. Patel defined the landmarks, and E. St. Clair placed them on the models.

5. Generating Procrustes distances between sets of OD landmarks. We calculated Procrustes distances between all pairs of specimens to generate dissimilarity matrices among specimens in each dataset, using 16 of the 18 landmarks for the tooth dataset, 11 landmarks for the first metatarsal dataset, and 13 landmarks for the radius.

6. Comparing Procrustes distances based on OD landmarks with distances based on GD correspondences. After generating dissimilarity matrices for OD landmark datasets we ran two analyses to compare them to the dissimilarity matrices generated by computing continuous Procrustes dissimilarity using the final mapping found by our correspondence algorithm. First we ran Mantel tests (15) to examine whether significant correlations existed between OD and GD based dissimilarity matrices. These were done using the statistical program PAST. Finally we used each dissimilarity matrix to run classification analyses. To taxonomically classify specimens using these matrices, we sequentially treated each model in our datasets as having unknown taxonomic affinities, and then identified it as belonging to the taxonomic group of its nearest neighbor (the specimen to which the Procrustes distance was the least). We considered only taxonomic groups of more than two specimens and performed this classification test for every specimen. We tallied the number of correct classifications and report them as a percentage of the total number of specimens in Table 1.

7. Topographic variable dataset for comparison to Procrustes distances in taxonomic and dietary classifications. Geometric morphometrics do not provide the only digital method used to quantify shape in biological sciences. Especially when it comes to teeth, the argument has been made that shape quantification will be less effective and more restrictive

in its applicability, if it is based on such detailed correspondence points [e.g., Boyer (1)]. To solve this problem, morphologists limit their assumptions about equivalence to the entire structure. That is, one would treat the crowns of two second-position molars as equivalent, but would not attempt to identify equivalent points on those two molars crowns. From here quantification proceeds by calculating averaged [Relief index: (1)], integrated [Dirichlet Normal Energy: (16)] or tallied [Orientation Patch Count: (17)] geometric properties of tooth crowns. These are often referred to as "topographic variables." Such variables are recognized as being most logically applicable to parsing variability due to differing dietary proclivities, as differently shaped teeth are suited for processing foods with differing mechanical properties. Furthermore, many biologists see such a goal as immanently more useful than determining taxonomic groups. As a result of such considerations we endeavored to test our algorithmic method against a dataset of several types of topographic variables and a more traditional diet-group determining variable.

For the 99 tooth models used in our other genus-level classifications (see supplementary table 4) we calculated shearing quotients, relief index, Dirichlet normal energy, and orientation patch count as described in Boyer (1), Bunn et al. (16) and Boyer et al. (17). We used the same neighbor joining classification method with these four variables (scaled to equal variance) defining Euclidean distances among specimens. Only 54% of the teeth were correctly classified (as compared to 91% using our cP algorithm or observer-based landmarks.

Conceding that taxonomic classification was never the proposed goal of topographic methods (and for some researchers not an interesting question), in our final classification analysis, we used a different grouping criterion – "dietary preference." We used the same nearest neighbor method to classify 74 extant tooth specimens with known diets into four dietary categories (frugivore, omnivore, folivore, and insectivore – see supplementary table 1). These dietary categories were previously defined and implemented in analyses presented by Boyer (1). We ran a total of 7 classification analyses using: 1) cP dissimilarity, 2) Euclidean distances defined by a combination of relief index, shearing quotient, Dirichlet normal energy, orientation patch count, and natural log molar length; 3) Euclidean distances defined by a combination of relief index, shearing quotient, Dirichlet normal energy, and orientation patch count; 4) Relief index alone; 5) shearing quotient alone; 6) Dirichlet normal energy alone; and 7) orientation patch count alone. See supplementary table 7 for results.

Supplementary Tables

Supplementary Table 1. Specimens for lower-molar study. Different highlights on 74 specimens represent different dietary proclivities: Yellow - insectivorous; green – folivorous; blue – omnivorous; fuchsia – frugivorous. Dietary assignments follow "diet code 1" of Boyer (1). Taxa with no highlight are fossils for which diet is unknown.

Specimen	Order	Family	Genus	Species
YPM 30440	Euprimates	Adapidae	*Adapis*	*Adapis parisiensis*
Qu 10966	Euprimates	Adapidae	*Adapis*	*Adapis parisiensis*
Q. I. 71	Euprimates	Adapidae	*Adapis*	*Adapis parisiensis*
Qu 11117	Euprimates	Adapidae	*Adapis*	*Adapis parisiensis*
PSS 7/20-8	Euprimates	Incertae sedis	*Altanius*	*Altanius orlovi*
PSS 20-58	Euprimates	Incertae sedis	*Altanius*	*Altanius orlovi*
MNHN Av 4854	Euprimates	Cercamonaiidae	*Donrussellia*	*Donrussellia gallica*
MNHN Av 7655	Euprimates	Cercamonaiidae	*Donrussellia*	*Donrussellia gallica*
MNHN Ri 170	Euprimates	Cercamonaiidae	*Donrussellia*	*Donrussellia provincialis*
CAB 04-274	Euprimates	Notharctidae	*Cantius*	*Cantius torresi*
UM 101958	Euprimates	Notharctidae	*Cantius*	*Cantius torresi*
UM 101958	Euprimates	Notharctidae	*Cantius*	*Cantius torresi*
UM 87852	Euprimates	Notharctidae	*Cantius*	*Cantius torresi*
CL 457	Euprimates	Omomyidae	*Teilhardina*	*Teilhardina belgica*
CL 455	Euprimates	Omomyidae	*Teilhardina*	*Teilhardina belgica*
IRSNB 4291	Euprimates	Omomyidae	*Teilhardina*	*Teilhardina belgica*
IRSNB M65	Euprimates	Omomyidae	*Teilhardina*	*Teilhardina belgica*
IRSNB M64	Euprimates	Omomyidae	*Teilhardina*	*Teilhardina belgica*
WL 128	Euprimates	Omomyidae	*Teilhardina*	*Teilhardina belgica*
WL 159	Euprimates	Omomyidae	*Teilhardina*	*Teilhardina belgica*
IRSNB 4296	Euprimates	Omomyidae	*Teilhardina*	*Teilhardina belgica*
SB-14	Euprimates	Megaladapidae	*Megaladapis*	*Megaladapis edwardsi*
AMNH 100832	Euprimates	Cheirogaleiidae	*Mirza*	*Mirza coquereli*
MCZ 45126	Euprimates	Cheirogaleiidae	*Mirza*	*Mirza coquereli*
AMNH 100830	Euprimates	Cheirogaleiidae	*Cheirogaleus*	*Cheirogaleus major*
AMNH 80072	Euprimates	Cheirogaleiidae	*Cheirogaleus*	*Cheirogaleus major*
AMNH 100654	Euprimates	Cheirogaleiidae	*Cheirogaleus*	*Cheirogaleus medius*
AMNH 174530	Euprimates	Cheirogaleiidae	*Microcebus*	*Microcebus griseorufus*
AMNH 174533	Euprimates	Cheirogaleiidae	*Microcebus*	*Microcebus griseorufus*
AMNH 174531	Euprimates	Cheirogaleiidae	*Microcebus*	*Microcebus griseorufus*
AMNH 174489	Euprimates	Cheirogaleiidae	*Microcebus*	*Microcebus griseorufus*
MCZ 44953	Euprimates	Cheirogaleiidae	*Phaner*	*Phaner furcifer*
AMNH 100829	Euprimates	Cheirogaleiidae	*Phaner*	*Phaner furcifer*
AMNH 119810	Euprimates	Galagidae	*Galago*	*Galago demidovii*
AMNH 241124	Euprimates	Galagidae	*Galago*	*Galago demidovii*
AMNH 239438	Euprimates	Galagidae	*Galago*	*Galago demidovii*
AMNH 241122	Euprimates	Galagidae	*Galago*	*Galago demidovii*
AMNH 187359	Euprimates	Galagidae	*Galago*	*Galago senegalensis*
AMNH 187362	Euprimates	Galagidae	*Galago*	*Galago zanzibaricus*
AMNH 187360	Euprimates	Galagidae	*Galago*	*Galago senegalensis*
AMNH 236379	Euprimates	Galagidae	*Galago*	*Galago alleni*
AMNH 241119	Euprimates	Galagidae	*Galago*	*Galago alleni*
AMNH 100635	Euprimates	Indridae	*Avahi*	*Avahi laniger*
USNM 83650	Euprimates	Indridae	*Avahi*	*Avahi laniger*
USNM 83652	Euprimates	Indridae	*Avahi*	*Avahi laniger*
AMNH 16699	Euprimates	Indridae	*Propithecus*	*Propithecus verreauxi*
AMNH 100827	Euprimates	Indridae	*Propithecus*	*Propithecus verreauxi*
USNM 257397	Euprimates	Indridae	*Propithecus*	*Propithecus verreauxi*
USNM 63349	Euprimates	Indridae	*Propithecus*	*Propithecus verreauxi*
USNM 63351	Euprimates	Indridae	*Propithecus*	*Propithecus diadema*
AMNH 100504	Euprimates	Indridae	*Indri*	*Indri indri*
AMNH 19159	Euprimates	Lemuridae	*Eulemur*	*Eulemur fulvus*
AMNH 18696	Euprimates	Lemuridae	*Eulemur*	*Eulemur fulvus*
USNM 063338	Euprimates	Lemuridae	*Eulemur*	*Eulemur fulvus*
USNM 063355	Euprimates	Lemuridae	*Hapalemur*	*Hapalemur griseus*
USNM 083668	Euprimates	Lemuridae	*Hapalemur*	*Hapalemur griseus*
BMNH 84.10.20.4	Euprimates	Lemuridae	*Hapalemur*	*Hapalemur simus*
AMNH 100598	Euprimates	Lemuridae	*Lemur*	*Lemur catta*
AMNH 100821	Euprimates	Lemuridae	*Lemur*	*Lemur catta*

AMNH 170743	Euprimates	Lemuridae	*Lemur*	*Lemur catta*
AMNH 170741	Euprimates	Lemuridae	*Lemur*	*Lemur catta*
AMNH 100514	Euprimates	Lemuridae	*Varecia*	*Varecia variegata*
AMNH 245092	Euprimates	Lemuridae	*Varecia*	*Varecia variegata*
AMNH 18041	Euprimates	Lemuridae	*Varecia*	*Varecia variegata*
AMNH 17338	Euprimates	Lemuridae	*Varecia*	*Varecia variegata*
AMNH 100612	Euprimates	Lepilemuridae	*Lepilemur*	*Lepilemur mustelinus*
AMNH 100642	Euprimates	Lepilemuridae	*Lepilemur*	*Lepilemur mustelinus*
AMNH 170576	Euprimates	Lepilemuridae	*Lepilemur*	*Lepilemur mustelinus*
AMNH 170578	Euprimates	Lepilemuridae	*Lepilemur*	*Lepilemur mustelinus*
AMNH 207949	Euprimates	Lorisidae	*Arctocebus*	*Arctocebus calabarensis*
AMNH 212954	Euprimates	Lorisidae	*Arctocebus*	*Arctocebus calabarensis*
USNM 511930	Euprimates	Lorisidae	*Arctocebus*	*Arctocebus calabarensis*
MCZ 38316	Euprimates	Lorisidae	*Arctocebus*	*Arctocebus calabarensis*
AMNH 150062	Euprimates	Lorisidae	*Loris*	*Loris tardigradus*
AMNH 240827	Euprimates	Lorisidae	*Loris*	*Loris tardigradus*
AMNH 217303	Euprimates	Lorisidae	*Loris*	*Loris tardigradus*
AMNH 87279	Euprimates	Lorisidae	*Nycticebus*	*Nycticebus bengalensis*
AMNH 101508	Euprimates	Lorisidae	*Nycticebus*	*Nycticebus javanicus*
AMNH 106650	Euprimates	Lorisidae	*Nycticebus*	*Nycticebus coucang*
AMNH 269860	Euprimates	Lorisidae	*Perodicticus*	*Perodicticus potto*
AMNH 31252	Euprimates	Lorisidae	*Perodicticus*	*Perodicticus potto*
IVPP 11001.1	Euprimates	Eosimiidae	*Eosimias*	*Eosimias centennias*
IVPP V10591	Euprimates	Eosimiidae	*Eosimias*	*Eosimias sinensis*
IVPP 11994	Euprimates	Eosimiidae	*Eosimias*	*Eosimias centennias*
IVPP 11001.2	Euprimates	Eosimiidae	*Eosimias*	*Eosimias centennias*
AMNH 109368	Euprimates	Tarsiidae	*Tarsius*	*Tarsius spectrum*
AMNH 109366	Euprimates	Tarsiidae	*Tarsius*	*Tarsius spectrum*
AMNH 196485	Euprimates	Tarsiidae	*Tarsius*	*Tarsius spectrum*
AMNH 106754	Euprimates	Tarsiidae	*Tarsius*	*Tarsius borneanus*
AMNH 106649	Euprimates	Tarsiidae	*Tarsius*	*Tarsius bancanus*
UALVP 43232	Primates	Plesiadapidae	*Pronothodectes*	*Pronothodectes matthewi*
UALVP 43276	Primates	Plesiadapidae	*Pronothodectes*	*Pronothodectes matthewi*
AMNH 35469	Primates	Plesiadapidae	*Pronothodectes*	*Pronothodectes matthewi*
AMNH 35462	Primates	Plesiadapidae	*Pronothodectes*	*Pronothodectes matthewi*
UMINN 1504	Primates	Purgatoriidae	*Purgatorius*	*Purgatorius unio*
UCMP 107406	Primates	Purgatoriidae	*Purgatorius*	*Purgatorius unio*
UM 90198	Primates	Purgatoriidae	*Purgatorius*	*Purgatorius titusi*
UM 90197	Primates	Purgatoriidae	*Purgatorius*	*Purgatorius titusi*
X	Primates	Chronolestidae	*Chronolestes*	*Chronolestes simul*
UALVP db194	Primates	Carpolestidae	*Elphidotarsius*	*Elphidotarsius russelli*
USNM 9545	Primates	Paromomyidae	*Paromomys*	*Paromomys maturus*
PU 14270	Primates	Palaechthonidae	*Plesiolestes*	*Plesiolestes problematicus*
UALVP 39498	Primates	Saxonellidae	*Saxonella*	*Saxonella naylori*
AMNH 120449	Dermoptera	Cynocephalidae	*Cynocephalus*	*Cynocephalus volans*
AMNH 107136	Dermoptera	Cynocephalidae	*Cynocephalus*	*Cynocephalus variegatus*
AMNH 203258	Dermoptera	Cynocephalidae	*Cynocephalus*	*Cynocephalus volans*
AMNH 24958	Dermoptera	Cynocephalidae	*Cynocephalus*	*Cynocephalus volans*
UMMZ 113339	Scandentia	Tupaiidae	*Tupaia*	*Tupaia montana*
UMMZ 123395	Scandentia	Tupaiidae	*Tupaia*	*Tupaia glis*
UMMZ 58984	Scandentia	Tupaiidae	*Tupaia*	*Tupaia glis*
Dummont specimen	Scandentia	Tupaiidae	*Tupaia*	*Tupaia glis*
USNM 488055	Scandentia	Ptilocercidae	*Ptilocercus*	*Ptilocercus lowii*
USNM 488059	Scandentia	Ptilocercidae	*Ptilocercus*	*Ptilocercus lowii*
CCM 71-8	Incertae sedis	Nyctitheriidae	*Leptacodon*	*Leptacodon sp.*
CCM 71-6	Incertae sedis	Nyctitheriidae	*Leptacodon*	*Leptacodon sp.*
CCM 73-31	Incertae sedis	Nyctitheriidae	*Leptacodon*	*Leptacodon sp.*

Supplementary Table 2. Specimens for first-metatarsal study

Specimen	"Superfamily"	Family	Genus	Species
AMNH 211487	Anthropoidea	Pitheciidae	*Callicebus*	*Callicebus donacophilus*
AMNH 211488	Anthropoidea	Pitheciidae	*Callicebus*	*Callicebus donacophilus*
AMNH 211489	Anthropoidea	Pitheciidae	*Callicebus*	*Callicebus donacophilus*
AMNH 211490	Anthropoidea	Pitheciidae	*Callicebus*	*Callicebus donacophilus*
AMNH 211493	Anthropoidea	Pitheciidae	*Callicebus*	*Callicebus donacophilus*
AMNH 211457	Anthropoidea	Cebidae	*Aotus*	*Aotus azarae*
AMNH 215050	Anthropoidea	Cebidae	*Aotus*	*Aotus azarae*
AMNH 215054	Anthropoidea	Cebidae	*Aotus*	*Aotus azarae*
AMNH 215056	Anthropoidea	Cebidae	*Aotus*	*Aotus azarae*
AMNH 215059	Anthropoidea	Cebidae	*Aotus*	*Aotus azarae*
AMNH 120386	Anthropoidea	Cercopithicidae	*Chlorocebus*	*Chlorocebus aethiops*
AMNH 187372	Anthropoidea	Cercopithicidae	*Chlorocebus*	*Chlorocebus aethiops*
AMNH 27705	Anthropoidea	Cercopithicidae	*Chlorocebus*	*Chlorocebus aethiops*
AMNH 54231	Anthropoidea	Cercopithicidae	*Chlorocebus*	*Chlorocebus aethiops*
AMNH 187392	Anthropoidea	Cercopithicidae	*Colobus*	*Colobus guereza*
AMNH 52206	Anthropoidea	Cercopithicidae	*Colobus*	*Colobus guereza*
AMNH 52229	Anthropoidea	Cercopithicidae	*Colobus*	*Colobus guereza*
AMNH 52248	Anthropoidea	Cercopithicidae	*Colobus*	*Colobus guereza*
AMNH 216247	Anthropoidea	Cercopithicidae	*Papio*	*Papio ursinus*
AMNH 80771	Anthropoidea	Cercopithicidae	*Papio*	*Papio ursinus*
SBU B	Anthropoidea	Cercopithicidae	*Papio*	*Papio ursinus*
SBU F	Anthropoidea	Cercopithicidae	*Papio*	*Papio ursinus*
SBU 5	Anthropoidea	Cercopithicidae	*Theropithecus*	*Theropithecus gelada*
AMNH 174408	Prosimii	Cheirogaleidae	*Microcebus*	*Microcebus griseorufus*
AMNH 174415	Prosimii	Cheirogaleidae	*Microcebus*	*Microcebus griseorufus*
AMNH 174423	Prosimii	Cheirogaleidae	*Microcebus*	*Microcebus griseorufus*
AMNH 185629	Prosimii	Cheirogaleidae	*Microcebus*	*Microcebus griseorufus*
AMNH 185630	Prosimii	Cheirogaleidae	*Microcebus*	*Microcebus griseorufus*
AMNH 150413	Prosimii	Galagidae	*Galagoides*	*Galagoides demidovii*
AMNH 212956	Prosimii	Galagidae	*Galagoides*	*Galagoides demidovii*
AMNH 212957	Prosimii	Galagidae	*Galagoides*	*Galagoides demidovii*
AMNH 212958	Prosimii	Galagidae	*Galagoides*	*Galagoides demidovii*
AMNH 215180	Prosimii	Galagidae	*Galagoides*	*Galagoides demidovii*
AMNH 201330	Prosimii	Galagidae	*Otolemur*	*Otolemur crassicadatus*
AMNH 216244	Prosimii	Galagidae	*Otolemur*	*Otolemur crassicadatus*
AMNH 245093	Prosimii	Galagidae	*Otolemur*	*Otolemur crassicadatus*
AMNH 80238	Prosimii	Galagidae	*Otolemur*	*Otolemur crassicadatus*
AMNH 80800	Prosimii	Galagidae	*Otolemur*	*Otolemur crassicadatus*
AMNH 80801	Prosimii	Galagidae	*Otolemur*	*Otolemur crassicadatus*
AMNH 170461	Prosimii	Indriidae	*Avahi*	*Avahi laniger*
AMNH 1155	Prosimii	Indriidae	*Propithecus*	*Propithecus diadema*
AMNH 170463	Prosimii	Indriidae	*Propithecus*	*Propithecus verreauxi*
AMNH 170471	Prosimii	Indriidae	*Propithecus*	*Propithecus verreauxi*
AMNH 170474	Prosimii	Indriidae	*Propithecus*	*Propithecus verreauxi*
AMNH 170491	Prosimii	Indriidae	*Propithecus*	*Propithecus verreauxi*
AMNH 257141	Prosimii	Indriidae	*Propithecus*	*Propithecus verreauxi*
AMNH 31255	Prosimii	Indriidae	*Propithecus*	*Propithecus verreauxi*
AMNH 170750	Prosimii	Lemuridae	*Eulemur*	*Eulemur fulvus*
AMNH 170755	Prosimii	Lemuridae	*Eulemur*	*Eulemur fulvus*
AMNH 170759	Prosimii	Lemuridae	*Eulemur*	*Eulemur fulvus*
AMNH 170764	Prosimii	Lemuridae	*Eulemur*	*Eulemur fulvus*
AMNH 150038	Prosimii	Lorisidae	*Loris*	*Loris tardigradus*
AMNH 269	Prosimii	Lorisidae	*Loris*	*Loris tardigradus*
AMNH 34257	Prosimii	Lorisidae	*Loris*	*Loris tardigradus*
AMNH 102027	Prosimii	Lorisidae	*Nycticebus*	*Nycticebus coucang*
AMNH 112990	Prosimii	Lorisidae	*Nycticebus*	*Nycticebus coucang*
AMNH 16591	Prosimii	Lorisidae	*Nycticebus*	*Nycticebus coucang*
AMNH 212953	Prosimii	Lorisidae	*Nycticebus*	*Nycticebus coucang*
AMNH 150414	Prosimii	Tarsiidae	*Tarsius*	*Tarsius syrichta*
AMNH 150448	Prosimii	Tarsiidae	*Tarsius*	*Tarsius philippensis*
AMNH 206757	Prosimii	Tarsiidae	*Tarsius*	*Tarsius syrichta*

Supplementary Table 3. Specimens for radius study

Specimen	Family	Genus	Species
SBU 01	Hominidae	*Homo*	*Homo sapiens*
SBU 02	Hominidae	*Homo*	*Homo sapiens*
SBU 04	Hominidae	*Homo*	*Homo sapiens*
SBU 05	Hominidae	*Homo*	*Homo sapiens*
SBU 06	Hominidae	*Homo*	*Homo sapiens*
SBU 07	Hominidae	*Homo*	*Homo sapiens*
SBU 08	Hominidae	*Homo*	*Homo sapiens*
SBU 09	Hominidae	*Homo*	*Homo sapiens*
SBU 10	Hominidae	*Homo*	*Homo sapiens*
SBU 11	Hominidae	*Homo*	*Homo sapiens*
MCZ 38018	Hominidae	*Pan*	*Pan paniscus*
MCZ 38019	Hominidae	*Pan*	*Pan paniscus*
MCZ 38020	Hominidae	*Pan*	*Pan paniscus*
SBU SUS1	Hominidae	*Pan*	*Pan paniscus*
SBU SUS2	Hominidae	*Pan*	*Pan troglodytes*
SBU KC1	Hominidae	*Pan*	*Pan troglodytes*
AIMUZ 10533	Hominidae	*Pan*	*Pan troglodytes*
AIMUZ 7127	Hominidae	*Pan*	*Pan troglodytes*
AIMUZ AS1595	Hominidae	*Pan*	*Pan troglodytes*
AIMUZ AS1810	Hominidae	*Pan*	*Pan troglodytes*
AMNH 167341	Hominidae	*Pan*	*Pan troglodytes*
AMNH 167344	Hominidae	*Pan*	*Pan troglodytes*
AMNH 51202	Hominidae	*Pan*	*Pan troglodytes*
AMNH 51376	Hominidae	*Pan*	*Pan troglodytes*
AMNH 51379	Hominidae	*Pan*	*Pan troglodytes*
AMNH 90191	Hominidae	*Pan*	*Pan troglodytes*
AIMUZ 7487	Hominidae	*Gorilla*	*Gorilla gorilla*
AIMUZ AS1690	Hominidae	*Gorilla*	*Gorilla gorilla*
AIMUZ PAL12	Hominidae	*Gorilla*	*Gorilla gorilla*
AMNH 167335	Hominidae	*Gorilla*	*Gorilla gorilla*
AMNH 167336	Hominidae	*Gorilla*	*Gorilla gorilla*
AMNH 167338	Hominidae	*Gorilla*	*Gorilla gorilla*
AMNH 167340	Hominidae	*Gorilla*	*Gorilla gorilla*
AMNH 54356	Hominidae	*Gorilla*	*Gorilla gorilla*
AMNH 90290	Hominidae	*Gorilla*	*Gorilla gorilla*
AIMUZ 1667	Pongidae	*Pongo*	*Pongo pygmaeus*
AIMUZ 8685	Pongidae	*Pongo*	*Pongo pygmaeus*
AIMUZ AS1531	Pongidae	*Pongo*	*Pongo pygmaeus*
AIMUZ AS1554	Pongidae	*Pongo*	*Pongo pygmaeus*
AMNH 140426	Pongidae	*Pongo*	*Pongo pygmaeus*
AMNH 200898	Pongidae	*Pongo*	*Pongo pygmaeus*
MCZ 37362	Pongidae	*Pongo*	*Pongo pygmaeus*
MCZ 37365	Pongidae	*Pongo*	*Pongo pygmaeus*
MCZ 50958	Pongidae	*Pongo*	*Pongo pygmaeus*
MCZ 50960	Pongidae	*Pongo*	*Pongo pygmaeus*

Supplementary Table 4. Classification success rates and failures, second mandibular molar. Individual rates (Ind) indicate percentage individuals correctly classified with other members of their order (Ord), family (Fam) and/or genus (Gen). "Ord", "Fam" and "Gen" rates are the average correct/total for each group (calculated this way, the varying sample size acquired for different orders, families and genera does not factor into the overall success rate). Incorrect assignments are given in the column to the left of the taxonomic classification of each specimen for which they occurred. Abbreviations: OD, observer determined (landmarks placed by E. St. Clair); GD, geometrically determined.

Classification Success Rates:		**111 correct / 116 total**	**110 correct / 116 total**		**100 correct / 106 total**	**98 correct / 106 total**		**91 correct / 99 total**	**90 correct / 99 total**
		Ind—95.7 Ord—87.0	Ind—94.8 Ord—88.6		Ind—94.3 Fam—92.9	Ind—92.5 Fam—93.3		Ind—91.9 Gen—89.9	Ind—90.9 Gen—89.2
Specimen	**Order**	**Order-OD**	**Order-GD**	**Family**	**Family-OD**	**Family-GD**	**Genus**	**Genus-OD**	**Genus-GD**
YPM 30440	Euprimates	--	--	Adapidae	--	--	*Adapis*	--	--
Qu 10966	Euprimates	--	--	Adapidae	--	--	*Adapis*	--	--
Q. I. 71	Euprimates	--	--	Adapidae	--	--	*Adapis*	--	--
Qu 11117	Euprimates	--	--	Adapidae	--	--	*Adapis*	--	--
PSS 7/20-8	Euprimates (*Altanius*)	--	--	NA	--	--	NA	--	--
PSS 20-58	Euprimates (*Altanius*)	--	--	NA	--	--	NA	--	--
MNHNAv4854	Euprimates	--	--	Cercamoninae	--	--	*Donrussellia*	--	--
MNHNAv7655	Euprimates	--	--	Cercamoninae	--	--	*Donrussellia*	--	--
MNHN Ri 170	Euprimates	--	--	Cercamoninae	*Cantius* UM101958	--	*Donrussellia*	*Cantius* UM101958	--
CAB 04-274	Euprimates	--	*Paromomys* USNM 9545	Notharctidae	--	--	*Cantius*	--	--
UM 101958	Euprimates	--	--	Notharctidae	--	--	*Cantius*	--	--
UM 101958	Euprimates	--	--	Notharctidae	--	--	*Cantius*	--	--
UM 87852	Euprimates	--	--	Notharctidae	--	--	*Cantius*	--	--
CL 457	Euprimates	--	--	Omomyidae	--	--	*Teilhardina*	--	--
CL 455	Euprimates	--	--	Omomyidae	--	--	*Teilhardina*	--	--
IRSNB 4291	Euprimates	--	--	Omomyidae	--	--	*Teilhardina*	--	--
IRSNB M65	Euprimates	--	--	Omomyidae	--	--	*Teilhardina*	--	--
IRSNB M64	Euprimates	--	--	Omomyidae	--	--	*Teilhardina*	--	--
WL 128	Euprimates	--	--	Omomyidae	--	--	*Teilhardina*	--	--
WL 159	Euprimates	--	--	Omomyidae	--	--	*Teilhardina*	--	--
IRSNB 4296	Euprimates	--	--	Omomyidae	--	--	*Teilhardina*	--	--
SB-14*	Euprimates (*Megaladapis*)	--	--	NA	--	--	NA	--	--
AMNH 100832	Euprimates	--	--	Cheirogaleidae (*Mirza*)	--	--	NA	--	--
MCZ 45126	Euprimates	--	--	Cheirogaleidae (*Mirza*)	--	--	NA	--	--
AMNH 100830	Euprimates	--	--	Cheirogaleiidae	--	--	*Cheirogaleus*	--	--
AMNH 80072	Euprimates	--	--	Cheirogaleiidae	--	--	*Cheirogaleus*	--	--
AMNH 100654	Euprimates	--	--	Cheirogaleiidae	--	--	*Cheirogaleus*	--	--
AMNH 174530	Euprimates	--	--	Cheirogaleiidae	--	--	*Microcebus*	--	--
AMNH 174533	Euprimates	--	--	Cheirogaleiidae	--	--	*Microcebus*	--	--
AMNH 174531	Euprimates	--	--	Cheirogaleiidae	--	--	*Microcebus*	--	--
AMNH 174489	Euprimates	--	--	Cheirogaleiidae	--	--	*Microcebus*	--	--
MCZ 44953	Euprimates	--	--	Cheirogaleidae (*Phaner*)	--	--	NA	--	--
AMNH 100829	Euprimates	--	--	Cheirogaleidae (*Phaner*)	--	--	NA	--	--
AMNH 119810	Euprimates	--	--	Galagidae	*Loris* AMH 217303	--	*Galago*	*Loris* AMH 217303	--
AMNH 241124	Euprimates	--	--	Galagidae	--	--	*Galago*	--	--
AMNH 239438	Euprimates	--	--	Galagidae	--	--	*Galago*	--	--
AMNH 241122	Euprimates	--	--	Galagidae	--	--	*Galago*	--	--
AMNH 187359	Euprimates	--	--	Galagidae	--	--	*Galago*	--	--
AMNH 187362	Euprimates	--	--	Galagidae	--	--	*Galago*	--	--
AMNH 187360	Euprimates	--	--	Galagidae	--	--	*Galago*	--	--
AMNH 236379	Euprimates	--	--	Galagidae	--	--	*Galago*	--	--
AMNH 241119	Euprimates	--	--	Galagidae	--	--	*Galago*	--	--
AMNH 100635	Euprimates	--	--	Indridae	--	--	*Avahi*	--	--
USNM 83650	Euprimates	--	--	Indridae	--	--	*Avahi*	--	--
USNM 83652	Euprimates	--	--	Indridae	--	--	*Avahi*	--	--
AMNH 16699	Euprimates	--	--	Indridae	--	--	*Propithecus*	--	--
AMNH 100827	Euprimates	--	--	Indridae	--	--	*Propithecus*	--	--
USNM 257397	Euprimates	--	--	Indridae	--	--	*Propithecus*	--	--
USNM 63349	Euprimates	--	--	Indridae	--	--	*Propithecus*	--	--
USNM 63351	Euprimates	--	--	Indridae	--	--	*Propithecus*	--	--
AMNH 100504	Euprimates	--	--	Indridae (*Indri*)	--	--	NA	--	--
AMNH 19159	Euprimates	--	--	Lemuridae	--	--	*Eulemur*	--	--
AMNH 18696	Euprimates	--	--	Lemuridae	--	--	*Eulemur*	--	--
USNM 063338	Euprimates	--	--	Lemuridae	--	--	*Eulemur*	Lemur AMNH170743	--
USNM 063355	Euprimates	--	--	Lemuridae	--	--	*Hapalemur*	--	--
USNM 083668	Euprimates	--	--	Lemuridae	--	*Adapis* Qu11117	*Hapalemur*	--	*Adapis* Qu11117
BMNH84.10.20.4	Euprimates	--	--	Lemuridae	*Microcebus* AMNH174533	*Nyctcebus* AMNH 106650	*Hapalemur*	*Microcebus* AMNH174533	*Nyctcebus* AMNH 106650
AMNH 100598	Euprimates	--	--	Lemuridae	--	--	*Lemur*	--	--
AMNH 100821	Euprimates	--	--	Lemuridae	--	--	*Lemur*	--	--
AMNH 170743	Euprimates	--	--	Lemuridae	--	--	*Lemur*	--	--
AMNH 170741	Euprimates	--	--	Lemuridae	--	--	*Lemur*	--	--
AMNH 100514	Euprimates	--	--	Lemuridae	--	--	*Varecia*	--	--
AMNH 245092	Euprimates	--	--	Lemuridae	--	--	*Varecia*	--	--
AMNH 18041	Euprimates	--	--	Lemuridae	--	--	*Varecia*	--	--
AMNH 17338	Euprimates	--	--	Lemuridae	--	--	*Varecia*	--	--
AMNH 100612	Euprimates	--	--	Lepilemuridae	--	--	*Lepilemur*	--	--
AMNH 100642	Euprimates	--	--	Lepilemuridae	--	--	*Lepilemur*	--	--
AMNH 170576	Euprimates	--	--	Lepilemuridae	--	--	*Lepilemur*	--	--
AMNH 170578	Euprimates	--	--	Lepilemuridae	--	--	*Lepilemur*	--	--
AMNH 207949	Euprimates	--	--	Lorisidae	--	--	*Arctocebus*	--	--
AMNH 212954	Euprimates	--	--	Lorisidae	--	--	*Arctocebus*	--	*Nyctcebus* AMNH 101508
USNM 511930	Euprimates	--	--	Lorisidae	--	*Adapis* YPM30440	*Arctocebus*	--	*Adapis* YPM30440
MCZ 38316	Euprimates	--	--	Lorisidae	--	--	*Arctocebus*	--	--
AMNH 150062	Euprimates	--	--	Lorisidae	--	--	*Loris*	--	--
AMNH 240827	Euprimates	--	--	Lorisidae	--	--	*Loris*	--	--
AMNH 217303	Euprimates	--	--	Lorisidae	*Galago* AMNH241119	--	*Loris*	*Galago* AMNH241119	--

AMNH 87279	Euprimates	--	--	Lorisidae	--	*Cantius* UM87852	*Nycticebus*	--	*Cantius* UM87852
AMNH 101508	Euprimates	--	--	Lorisidae	--	*Donrussellia* MNHN Av7655	*Nycticebus*	*Arctocebus* AMNH212954	*Donrussellia* MNHN Av7655
AMNH 106650	Euprimates	--	--	Lorisidae	--	--	*Nycticebus*	--	--
AMNH 269860	Euprimates	--	--	Lorisidae	--	--	*Perodicticus*	--	--
AMNH 31252	Euprimates	--	--	Lorisidae	--	--	*Perodicticus*	--	--
IVPP 11001.1	Euprimates	--	--	Eosimiidae	--	--	*Eosimias*	--	--
IVPP V10591	Euprimates	--	--	Eosimiidae	--	--	*Eosimias*	--	--
IVPP 11994	Euprimates	--	--	Eosimiidae	--	--	*Eosimias*	--	--
IVPP 11001.2	Euprimates	--	--	Eosimiidae	--	--	*Eosimias*	--	--
AMNH 109368	Euprimates	--	--	Tarsiidae	--	--	*Tarsius*	--	--
AMNH 109366	Euprimates	--	--	Tarsiidae	--	--	*Tarsius*	--	--
AMNH 196485	Euprimates	--	--	Tarsiidae	--	--	*Tarsius*	--	--
AMNH 106754	Euprimates	--	--	Tarsiidae	--	--	*Tarsius*	--	--
AMNH 106649	Euprimates	--	--	Tarsiidae	--	--	*Tarsius*	--	--
UALVP 43232	Primates	--	--	Plesiadapidae	--	--	*Pronothodectes*	--	--
UALVP 43276	Primates	--	--	Plesiadapidae	--	--	*Pronothodectes*	--	--
AMNH 35469	Primates	--	--	Plesiadapidae	--	--	*Pronothodectes*	--	--
AMNH 35462	Primates	--	--	Plesiadapidae	--	--	*Pronothodectes*	--	--
UMINN 1504	Primates	--	*Leptacodon* CCM 71-6	Purgatoriidae	--	*Leptacodon* CCM 71-6	*Purgatorius*	--	*Leptacodon* CCM 71-6
UCMP 107406	Primates	--	*Leptacodon* CCM 71-6	Purgatoriidae	--	*Leptacodon* CCM 71-6	*Purgatorius*	--	*Leptacodon* CCM 71-6
UM 90198	Primates	--	--	Purgatoriidae	--	--	*Purgatorius*	--	--
UM 90197	Primates	*Leptacodon* CCM 71-6	--	Purgatoriidae	*Leptacodon* CCM 71-6	--	*Purgatorius*	*Leptacodon* CCM 71-6	--
IVPPV10696.2-	Primates (*Chronolestes*)	*Teilhardina* IRSNBm65	--	NA	--	--	NA	--	--
UALVP db194	Primates (*Elphidotarsius*)	--	--	NA	--	--	NA	--	--
USNM 9545	Primates (*Paromomys*)	*Teilhardina* IRSNBm65	*Cantius* CAB04274	NA	--	--	NA	--	--
PU 14270	Primates (*Plesiolestes*)	*Leptacodon* CCM 71-6	*Leptacodon* CCM 71-6	NA	--	--	NA	--	--
UALVP 39498	Primates (*Saxonella*)	--	--	NA	--	--	NA	--	--
AMNH 120449	Dermoptera	--	--	Cynocephalidae	--	--	*Cynocephalus*	--	--
AMNH 107136	Dermoptera	--	*Galago* AMNH18736	Cynocephalidae	--	*Galago* AMNH18736	*Cynocephalus*	--	*Galago* AMNH18736
AMNH 203258	Dermoptera	--	--	Cynocephalidae	--	--	*Cynocephalus*	--	--
AMNH 24958	Dermoptera	--	--	Cynocephalidae	--	--	*Cynocephalus*	--	--
UMMZ 113339	scandentia	--	--	Tupaiidae	--	--	*Tupaia*	--	--
UMMZ 123395	scandentia	--	--	Tupaiidae	--	--	*Tupaia*	--	--
UMMZ 58984	scandentia	--	--	Tupaiidae	--	--	*Tupaia*	--	--
Dummont specimen	scandentia	--	--	Tupaiidae	--	--	*Tupaia*	--	--
USNM 488055	Scandentia (*Ptilocercus*)	--	--	NA	--	--	NA	--	--
USNM 488059	Scandentia (*Ptilocercus*)	--	--	NA	--	--	NA	--	--
CCM 71-8	Incertae sedis	--	--	Nyctitheriidae	--	--	*Leptacodon*	--	--
CCM 71-6	Incertae sedis	*Purgatorius* UM90197	--	Nyctitheriidae	*Purgatorius* UM90197	--	*Leptacodon*	*Purgatorius* UM90197	--
CCM 73-31	Incertae sedis	--	--	Nyctitheriidae	--	--	*Leptacodon*	--	--

Supplementary Table 5. Classification success rates and failures, proximal first metatarsal. The computer GD correspondences yielded classification success rates much higher than OD landmarks from observer 2 (E. St. Clair) in this case. However, the computer was slightly les successful than OD landmarks from observer 1 (D. M. Boyer). There were no mistakes at the level of Anthropoidea vs. Prosimii by anyone. See Supplementary Table 5 for more explanation and definitions of abbreviations.

Classification success rates		**57 correct / 61 total**	**56 correct / 61 total**	**51 correct / 61 total**		**52 correct / 59 total**	**48 correct / 59 total**	**44 correct / 59 total**
		Ind--93.4 Fam—94.2	Ind--91.8 Fam--91.4	Ind--83.6 Fam--82.4		Ind—88.1 Fam--87.7	Ind--81.3 Gen--82.0	Ind--74.5 Gen--75.6
specimen	**Family**	**Family-OD1**	**Family-GD**	**Family-OD2**	**Genus**	**Genus-OD1**	**Genus-GD**	**Genus-OD2**
AMNH 211487	Atelidae	--	--	--	*Callicebus*	--	--	--
AMNH 211488	Atelidae	--	--	--	*Callicebus*	--	--	--
AMNH 211489	Atelidae	--	--	--	*Callicebus*	--	--	--
AMNH 211490	Atelidae	--	--	--	*Callicebus*	--	--	--
AMNH 211493	Atelidae	--	--	--	*Callicebus*	--	--	--
AMNH 211457	Cebidae	*Colobus* AMNH 211487	--	--	*Aotus*	*Colobus* AMNH 211487	--	--
AMNH 215050	Cebidae	--	--	--	*Aotus*	--	--	--
AMNH 215054	Cebidae	--	--	--	*Aotus*	--	--	--
AMNH 215056	Cebidae	--	*Papio* SBU PuF	--	*Aotus*	--	*Papio* SBU PuF	--
AMNH 215059	Cebidae	--	--	--	*Aotus*	--	--	--
AMNH 120386	Cercopithicidae	--	--	--	*Chlorocebus*	*Papio* SBU PuB	--	--
AMNH 187372	Cercopithicidae	--	--	--	*Chlorocebus*	--	--	--
AMNH 27705	Cercopithicidae	--	--	--	*Chlorocebus*	--	*Papio* SBU PuF	--
AMNH 54231	Cercopithicidae	--	--	--	*Chlorocebus*	--	--	--
AMNH 52206	Cercopithicidae	--	--	--	*Colobus*	*Papio* AMNH 216247	*Papio* SBU PuB	*Papio* AMNH 216247
AMNH 52229	Cercopithicidae	--	--	--	*Colobus*	--	--	*Chlorocebus* AMNH 187372
AMNH 52248	Cercopithicidae	--	--	--	*Colobus*	--	*Papio* AMNH 80771	--
AMNH 187392	Cercopithicidae	--	--	*Aotus* AMNH 215056	*Colobus*	*Papio* AMNH 216247	--	*Aotus* AMNH 215056
AMNH 216247	Cercopithicidae	--	--	--	*Papio*	--	--	*Colobus* AMNH 52206
AMNH 80771	Cercopithicidae	--	--	--	*Papio*	--	--	*Colobus* AMNH 52206
SBU PuB	Cercopithicidae	--	--	--	*Papio*	--	*Colobus* AMNH 52206	--
SBU PuF	Cercopithicidae	--	--	--	*Papio*	*Colobus* AMNH 52206	--	--
SBU Tg5	Cercopithicidae	--	--	--	*Theropithecus*	na	na	na
AMNH 174408	Cheirogaleidae	--	*Eulemur* AMNH 170764	--	*Microcebus*	--	*Eulemur* AMNH 170764	--
AMNH 174415	Cheirogaleidae	--	--	--	*Microcebus*	--	--	--
AMNH 174423	Cheirogaleidae	--	--	*Eulemur* AMNH 170755	*Microcebus*	--	--	*Eulemur* AMNH 170755
AMNH 185629	Cheirogaleidae	--	--	--	*Microcebus*	--	--	--
AMNH 185630	Cheirogaleidae	--	--	--	*Microcebus*	--	--	--
AMNH 150413	Galagidae	--	--	--	*Galagoides*	--	*Otolemur* AMNH 216244	--
AMNH 212956	Galagidae	*Microcebus* AMNH 185630	--	--	*Galagoides*	*Microcebus* AMNH 185630	*Otolemur* AMNH 216244	--
AMNH 212957	Galagidae	--	--	--	*Galagoides*	--	*Otolemur* AMNH 80801	--
AMNH 212958	Galagidae	--	--	--	*Galagoides*	--	--	--

AMNH 215180	Galagidae	*Microcebus* AMNH 185629	*Microcebus* AMNH 185630	*Microcebus* AMNH 174423	*Galagoides*	*Microcebus* AMNH 185629	*Microcebus* AMNH 185630	*Microcebus* AMNH 174423
AMNH 201330	Galagidae	--	--	--	*Otolemur*	--	--	--
AMNH 216244	Galagidae	--	--	--	*Otolemur*	--	--	--
AMNH 245093	Galagidae	--	--	--	*Otolemur*	--	--	--
AMNH 80238	Galagidae	--	--	--	*Otolemur*	--	--	--
AMNH 80800	Galagidae	--	--	--	*Otolemur*	--	--	--
AMNH 80801	Galagidae	--	--	--	*Otolemur*	--	--	--
AMNH 170461	Indriidae	*Eulemur* AMNH 170755	*Eulemur* AMNH 170755	*Eulemur* AMNH 170759	*Avahi*	na	na	na
AMNH 1155	Indriidae	--	*Eulemur* AMNH 170759	--	*Propithecus*	--	*Eulemur* AMNH 170759	
AMNH 170463	Indriidae	--	--	*Eulemur* AMNH 170750	*Propithecus*	--	--	*Eulemur* AMNH 170750
AMNH 170471	Indriidae	--	--	*Eulemur* AMNH 170759	*Propithecus*	--	--	*Eulemur* AMNH 170759
AMNH 170474	Indriidae	--	--	--	*Propithecus*	--	--	--
AMNH 170491	Indriidae	--	--	--	*Propithecus*	--	--	--
AMNH 257141	Indriidae	--	--	*Eulemur* AMNH 170759	*Propithecus*	--	--	*Eulemur* AMNH 170759
AMNH 31255	Indriidae		--		*Propithecus*		--	--
AMNH 170750	Lemuridae	--	--	*Propithecus* AMNH 170463	*Eulemur*	--	--	*Propithecus* AMNH 170463
AMNH 170755	Lemuridae	--	--	*Microcebus* AMNH 174423	*Eulemur*	--	--	*Microcebus* AMNH 174423
AMNH 170759	Lemuridae	--	--	--	*Eulemur*	--	--	--
AMNH 170764	Lemuridae	--	--	--	*Eulemur*	--	--	--
AMNH 150038	Lorisidae	--	--	--	*Loris*	--	--	
AMNH 269	Lorisidae	--	--	--	*Loris*	--	--	*Nycticebus* AMNH 102027
AMNH 34257	Lorisidae	--	--	--	*Loris*		--	--
AMNH 102027	Lorisidae	--	--	--	*Nycticebus*	--	--	--
AMNH 112990	Lorisidae	--	--	--	*Nycticebus*	--	--	--
AMNH 16591	Lorisidae	--	--	*Eulemur* AMNH 170755	*Nycticebus*	--	--	*Eulemur* AMNH 170755
AMNH 212953	Lorisidae	--	--	--	*Nycticebus*	--	--	--
AMNH 150414	Tarsiidae	--	--	--	*Tarsius*	--	--	--
AMNH 150448	Tarsiidae	--	--	--	*Tarsius*	--	--	--
AMNH 206757	Tarsiidae	--	--	--	*Tarsius*	--	--	--

Supplementary Table 6. Classification success rates and failures, distal radius. GD correspondences yielded the highest classification success rates as compared to OD landmarks (defined by B. A. Patel and placed by E. St. Clair). Because this sample was more taxonomically restricted than others, only genus level success rates are reported. See Supplementary Table 5 for more explanation and definitions of abbreviations. Only incorrect nearest neighbors are in the right-most columns.

Classification Success Rates			**36 correct / 45 total**	**39 correct / 45 total**
			Ind--80.0, Gen--82.8	Ind--86.6, Gen--87.8
Specimen	**Family**	**Genus**	**Genus-OD**	**Genus-GD**
SBU 01	Hominidae	*Homo*	--	--
SBU 02	Hominidae	*Homo*	--	--
SBU 04	Hominidae	*Homo*	--	--
SBU 05	Hominidae	*Homo*	--	--
SBU 06	Hominidae	*Homo*	--	--
SBU 07	Hominidae	*Homo*	--	--
SBU 08	Hominidae	*Homo*	--	--
SBU 09	Hominidae	*Homo*	--	--
SBU 10	Hominidae	*Homo*	--	--
SBU 11	Hominidae	*Homo*	--	--
MCZ 38018	Hominidae	*Pan paniscus*	--	--
MCZ 38019	Hominidae	*Pan paniscus*	*Pan trog* AMNH 51376	*Pan trog* AMNH 51376
MCZ 38020	Hominidae	*Pan paniscus*	--	--
SBU SUS1	Hominidae	*Pan trog*	*Pan trog* MCZ 38020	--
SBU SUS2	Hominidae	*Pan trog*	--	--
SBU KC1	Hominidae	*Pan paniscus*	*Pan trog* AMNH 167344	*Pan trog* AMNH 51376
AIMUZ 10533	Hominidae	*Pan trog*	--	*Gorilla* AMNH 167340
AIMUZ 7127	Hominidae	*Pan trog*	--	--
AIMUZ AS1595	Hominidae	*Pan trog*	*Pongo* AIMUZ 8685	--
AIMUZ AS1810	Hominidae	*Pan trog*	--	--
AMNH 167341	Hominidae	*Pan trog*	*Gorilla* AIMUZ 7487	--
AMNH 167344	Hominidae	*Pan trog*	--	--
AMNH 51202	Hominidae	*Pan trog*	--	--
AMNH 51376	Hominidae	*Pan trog*	--	--
AMNH 51379	Hominidae	*Pan trog*	--	--
AMNH 90191	Hominidae	*Pan trog*	*Pan trog* MCZ 38020	--
AIMUZ 7487	Hominidae	*Gorilla*	--	--
AIMUZ AS1690	Hominidae	*Gorilla*	--	--
AIMUZ PAL12	Hominidae	*Gorilla*	--	--
AMNH 167335	Hominidae	*Gorilla*	--	--
AMNH 167336	Hominidae	*Gorilla*	--	--
AMNH 167338	Hominidae	*Gorilla*	*Pan* AMNH 167341	--
AMNH 167340	Hominidae	*Gorilla*	--	--
AMNH 54356	Hominidae	*Gorilla*	--	--
AMNH 90290	Hominidae	*Gorilla*	--	--
AIMUZ 1667	Pongidae	*Pongo*	--	*Pan trog* AMNH 90191
AIMUZ 8685	Pongidae	*Pongo*	--	--
AIMUZ AS1531	Pongidae	*Pongo*	--	--
AIMUZ AS1554	Pongidae	*Pongo*	--	*Pan trog* AMNH 90191
AMNH 140426	Pongidae	*Pongo*	--	*Pan paniscus* SBU KC1
AMNH 200898	Pongidae	*Pongo*	*Pan* AIMUZ 7127	--
MCZ 37362	Pongidae	*Pongo*	--	--
MCZ 37365	Pongidae	*Pongo*	--	--
MCZ 50958	Pongidae	*Pongo*	*Pan trog* AIMUZ AS1810	--
MCZ 50960	Pongidae	*Pongo*		--

Supplementary Table 7. Comparison of taxonomic and dietary classification success rates for analyses of teeth using topographic variables, and automatically determined Procrustes distances.

Classification	cP	Topo1	Topo2*	RFI	SQ	DNE	OPC
Genus-group	90/99	54/99	NA	NA	NA	NA	NA
Diet-group	69/74	59/74	69/74	53/74	34/74	28/74	31/74

Legend:
cP – automatically determined Procrustes distance
Topo1 – combination of four variables RFI, SQ, DNE, OPC
Topo2 – combination of five variables RFI, SQ, DNE, OPC, lnM2 length
RFI – relief index
SQ – shearing quotient
DNE – dirichlet normal energy
OPC – orientation patch count
***Analysis is not strictly limited to shape data. Inclusion of ln (natural logarithm) of M2 (second lower molar) length is considered absolute size data.**

Supplementary Table 8. Landmark Propagation Error summary statistics

group	mean cP-distance	distribution of discrete Procrustes distance for propagated landmarks versus "ground-truth" landmarks:						
		mean	standard deviation	median	quartiles		extremes	
smallest 100	0.04	0.034	0.009	0.033	0.028	0.040	0.017	0.056
"middle" 100	0.1	0.072	0.017	0.070	0.057	0.084	0.035	0.122
"largest" 100	0.21	0.129	0.035	0.126	0.111	0.143	0.070	0.285

Supplementary Figures

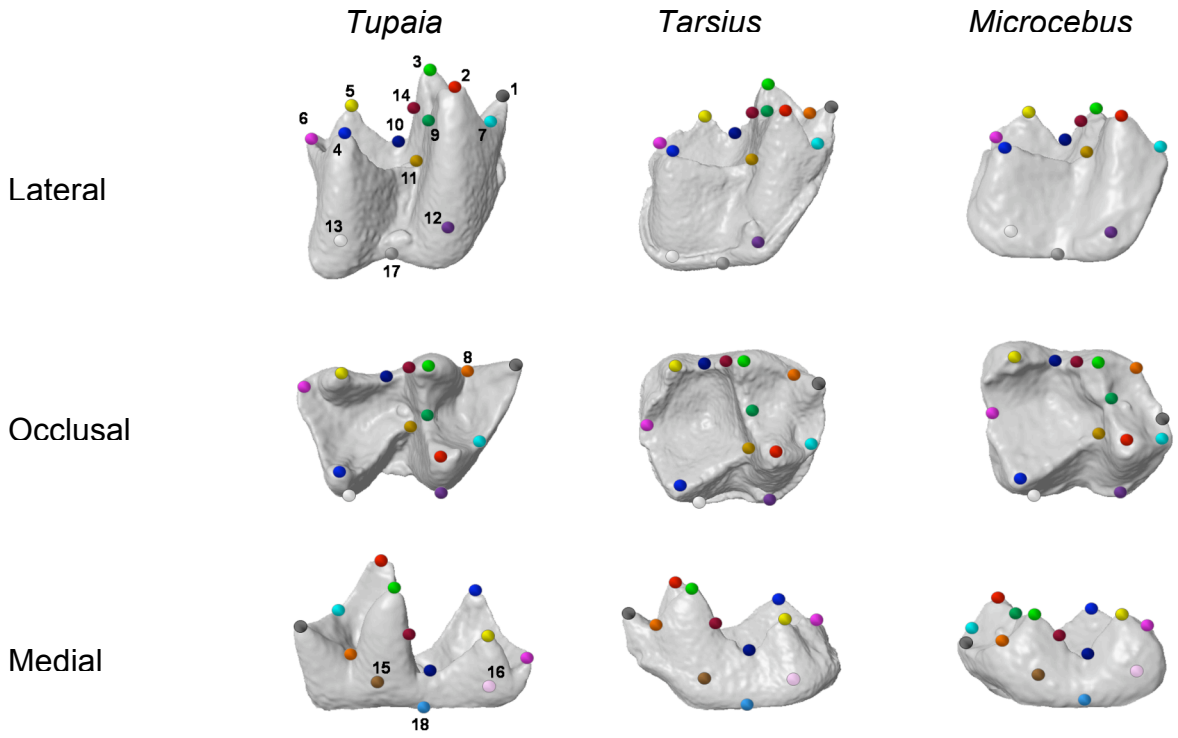

Supplementary Figure 1. Eighteen observer (E. St. Clair) defined landmarks illustrated on teeth of three different taxa in three different views. Points were selected to a) delineate molar features (cusps and crests) commonly described in comparative analyses of mammalian dental morphology, b) capture variation in crest curvature, and c) represent landmarks used as endpoints in linear measurements in quantitative analyses of dental variation. The observer determined points are illustrated in Figure S1 and defined below. Only points 1-16 were used to create the distance matrix used for the discrimination of taxa. The program Landmark Editor was used to collect these datapoints. Landmark descriptions: **1**, anterior terminus of the paracristid (crest issuing antero-lingually from the protoconid); equivalent to paraconid when latter is present; **2**, protoconid; **3**, metaconid; **4**, hypoconid; **5**, entoconid; **6**, posterior terminus of the hypocristid (crest issuing postero-lingually from the hypoconid); **7**, point of reflection (apex of curvature) of the paracristid; **8**, notch anterior to metaconid; **9**, notch between metaconid and protoconid; **10**, talonid notch (deepest point between metaconid and entoconid); **11**, contact of cristid obliqua (crest issuing antero-lingually from hypoconid) and the trigonid; **12**, most buccal point on the trigonid; **13**, most buccal point on the talonid; **14**, midpoint of metacristid (crest issuing posteriorly from metaconid); **15**, most lingual point on trigonid; **16**, most lingual point on talonid; **17**, buccal intersection of crown base and the trigonid-talonid contact; **18**, lingual intersection of crown base and the trigonid-talonid contact.

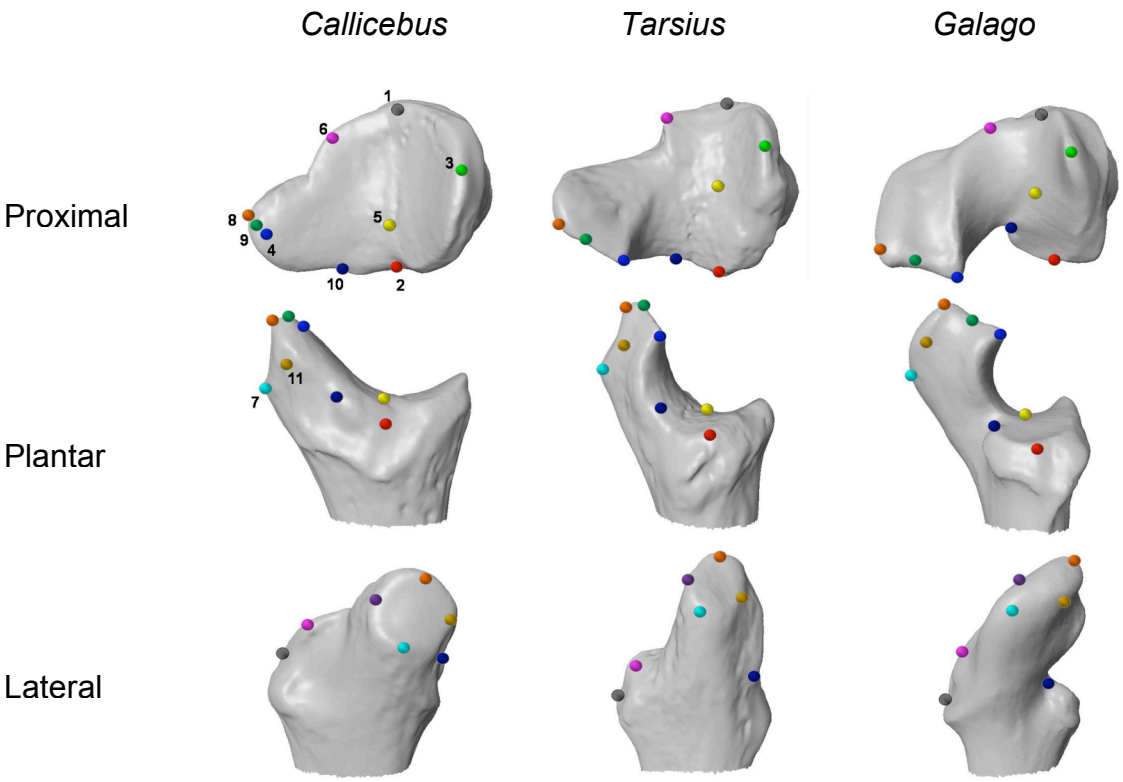

Supplementary Figure 2A, Fourteen observer (D. M. Boyer) defined landmarks illustrated on teeth of three different taxa in three different views. Only 1-11 were used in analyses for standardization to observer two (Fig. 2B). The program Landmark Editor was used to collect these datapoints **1**, dorsal-most margin of proximal articular surface; **2**, ventral-most margin of proximal articular surface; **3**, On most specimens the dorsomedial corner of the proximal articular facet is peaked (squared). This landmark resides in this corner. If no such convexity exists the landmark shall reside at the midpoint between #1 and #2; **4**, proximal-most point of lateral margin of proximal articular surface (peroneal tubercle apex); **5**, In most specimens there is convexity to the proximal articular surface in the dorsal ventral direction, and a concavity in the mediolateral direction. This landmark is defined as the residing at the maximum and minimum of these two curves, respectively; **6**, On most specimens the dorsolateral corner of the proximal articular facet is peaked (squared). This landmark resides in this corner. If no such convexity exists the landmark shall reside at the end of the first third of the distance from #1 to #4; **7**, distal apex of the attachment area for peroneous longus muscle's tendon, typically a flattened area on lateral surface of peroneal tubercle; **8**, proximal apex of the attachment area for peroneous longus muscle's tendon, typically a flattened area on lateral surface of peroneal tubercle; **9**, most proximally projecting peak between #4 and #8, or midpoint; **10**, In most specimens there is concavity, or even a notch in the ventrolateral corner of the proximal facet, in which this landmark resides. If no such concavity exists, the landmark shall reside at the midpoint between #2 and #4; **11**, In most specimens there is a flattened area on the tip of the peroneal process representing the attachment of the peroneous longus tendon. This landmark represents the ventral extreme of this flattened area; **12**, In most specimens there is a flattened area on the tip of the peroneal process representing the attachment of the peroneous longus tendon. This landmark represents the dorsal extreme of this flattened area; **13**, Along the ventromedial margin of the proximal articular facet there is often a notch. This landmark resides in that notch; **14**, On the medial aspect of the proximal end just distal to the rim of the proximal articular surface, there is a raised lip. In some taxa this lip is concentrated into one or two tubercles. The landmark is the peak of the more dorsal of the two tubercles, or the peak of the ridge corresponding to where the more dorsal of the tubercles would be if it is absent.

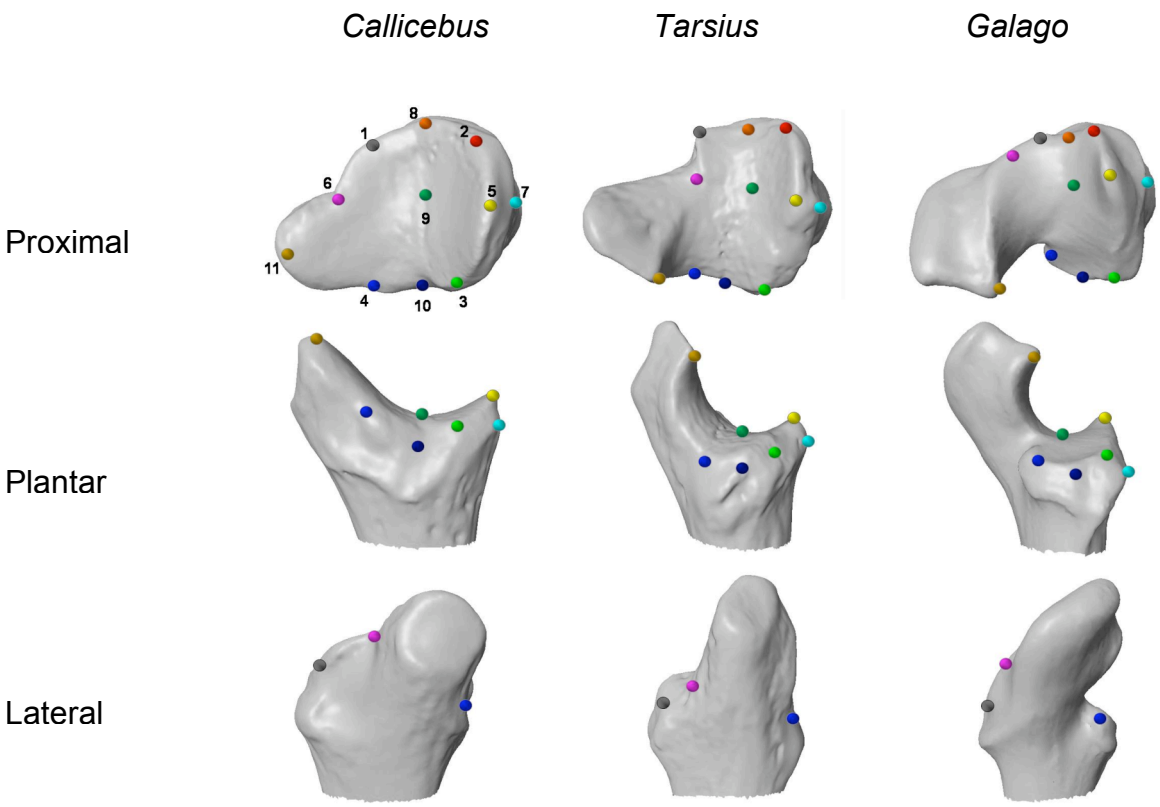

Supplementary Figure 2B. Eleven landmarks defined by a second observer (E. St. Clair) illustrated on teeth of same three taxa and views. The program Landmark Editor was used to collect these datapoints. **1**, dorsomedial limit of joint surface in proximal view; **2**, dorsolateral limit of joint surface in proximal view; **3**, ventrolateral limit of joint surface in proximal view; **4**, ventromedial limit of joint surface in proximal view; **5**, most proximal point on medial joint surface margin (apex of dorsoventral curvature); **6**, dorsal limit (base) of peroneal tuberosity; **7**, most lateral point on proximal metatarsal; **8**, midpoint between #1 and #2; **9**, intersection of the midline of the medio-lateral and dorso-ventral curvature (usually positioned between #5 and #6; **10**, midpoint between #3 and #4; **11**, most proximal point on lateral joint surface margin.

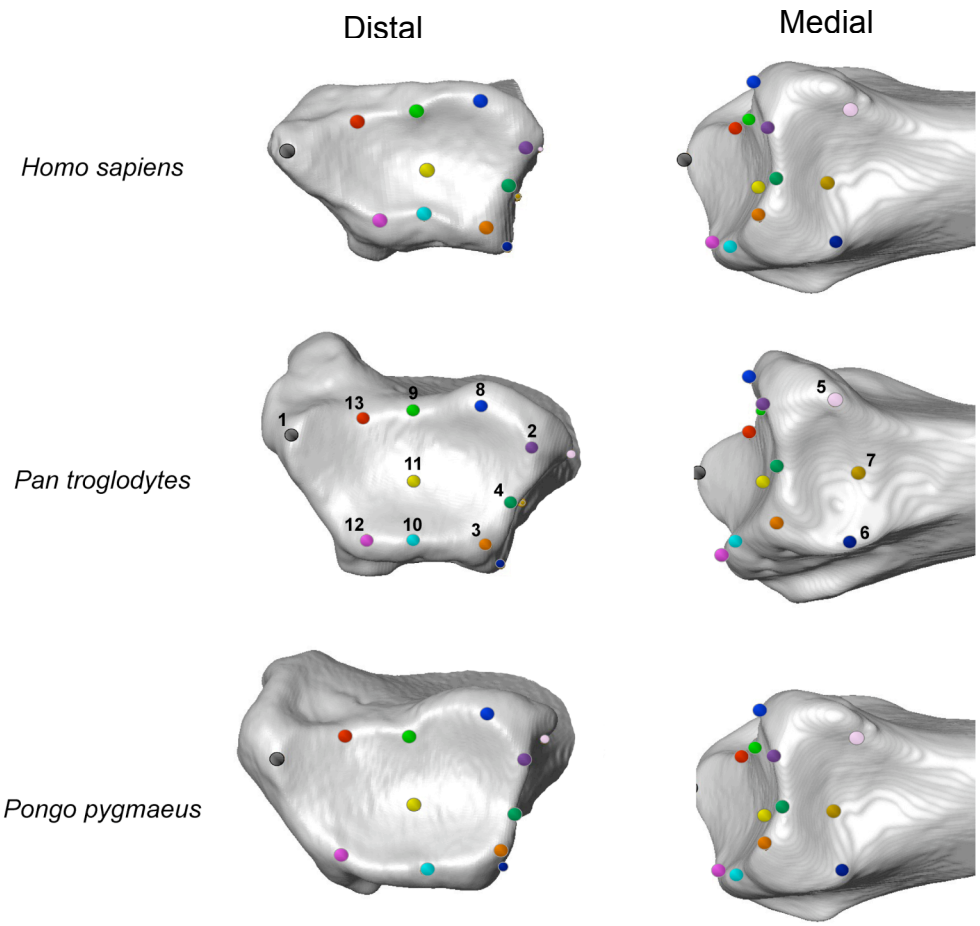

Supplementary Figure 3. Thirteen observer defined landmarks (defined by B. A. Patel, collected by E. St. Clair) illustrated on distal radii of three different taxa in two different views. The program Landmark Editor was used to collect these datapoints. Landmark descriptions: **1**, Lateral-most extent of the distal articular surface (approximates the lateral styloid process). Thys is typically the most distal point of the radius when positioned in anatomical position **2**, Ventromedial corner of the distal articular surface (Could also be called the ventrodistal corner of the ulnar articular surface on the medial side of the distal radius); **3**, Dorsomedial corner of the distal articular surface (Could also be called the dorsoodistal corner of the ulnar articular surface on the medial side of the distal radius); **4**, Deepest point between Landmarks 2 and 3 along the lateral aspect of the distal articular surface. Should approximate the center between Landmarks 2 and 3; **5**, Ventroproximal corner of the ulnar articular surface (on the medial side of the distal radius); **6**, Dorsoproximal corner of the ulnar articular suface (on the medlal side of the distal radiius); **7**, Center of the proximal margin of the ulnar articular surface (on the medial side of the distal radius) appoximately between Landmarks 5 and 6; **8**, Ventral most extent of the distal articular surface (usually should be located on the medial side of the distal articular surface). This is also the ventral most point of the lunate surface region; **9**, Approximates the junction between the scaphoid and lunate surface regions on the ventral side of the distal articular surface. Typically, there is a notch here or is the termination of the central ridge; **10**, Approximates the junction between the scaphoid and lunate surface regions on the dorsal side of the distal articular surface. Typically, there is a notch here or is the termination of the central ridge; **11**, Center of the distal articular surface (usually the deepest point, but sometimes there is a ridge of bone there approximating the separation of the scaphoid and lunate surface regions). Should line up between Landmarks 9 and 10; **12**, A notch on the dorsolateral (scaphoid surface region) side of the distal articular surface located somewhere between Landmarks 1 and 10; **13**, A notch on the ventrolateral (scaphoid surface region) side of the distal articular surface located somewhere between Landmarks 1 and 9.

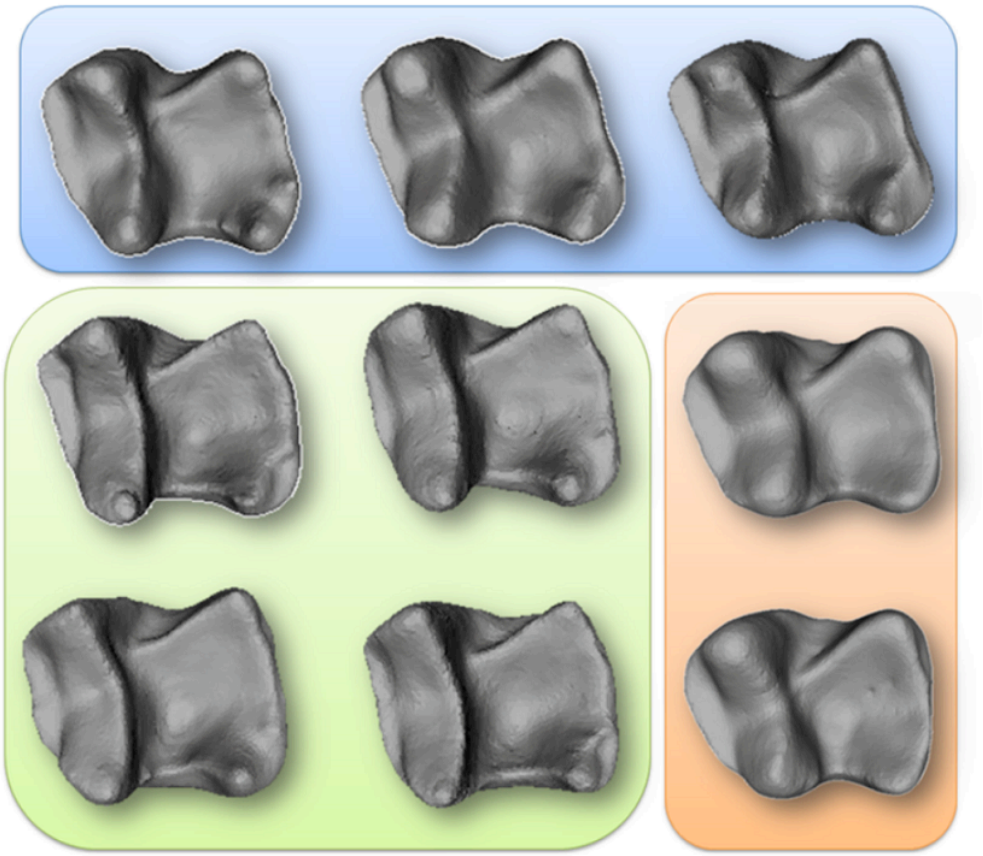

Supplementary Figure 4. Species groups for *Galago* from the dental dataset. All individuals were correctly classified to the appropriate species-group using the leaveone-out nearest neighbor classification method of this study. Orange – *Galago alleni*; Green – *Galago demidovii*; Blue – *Galago senegalensis*.

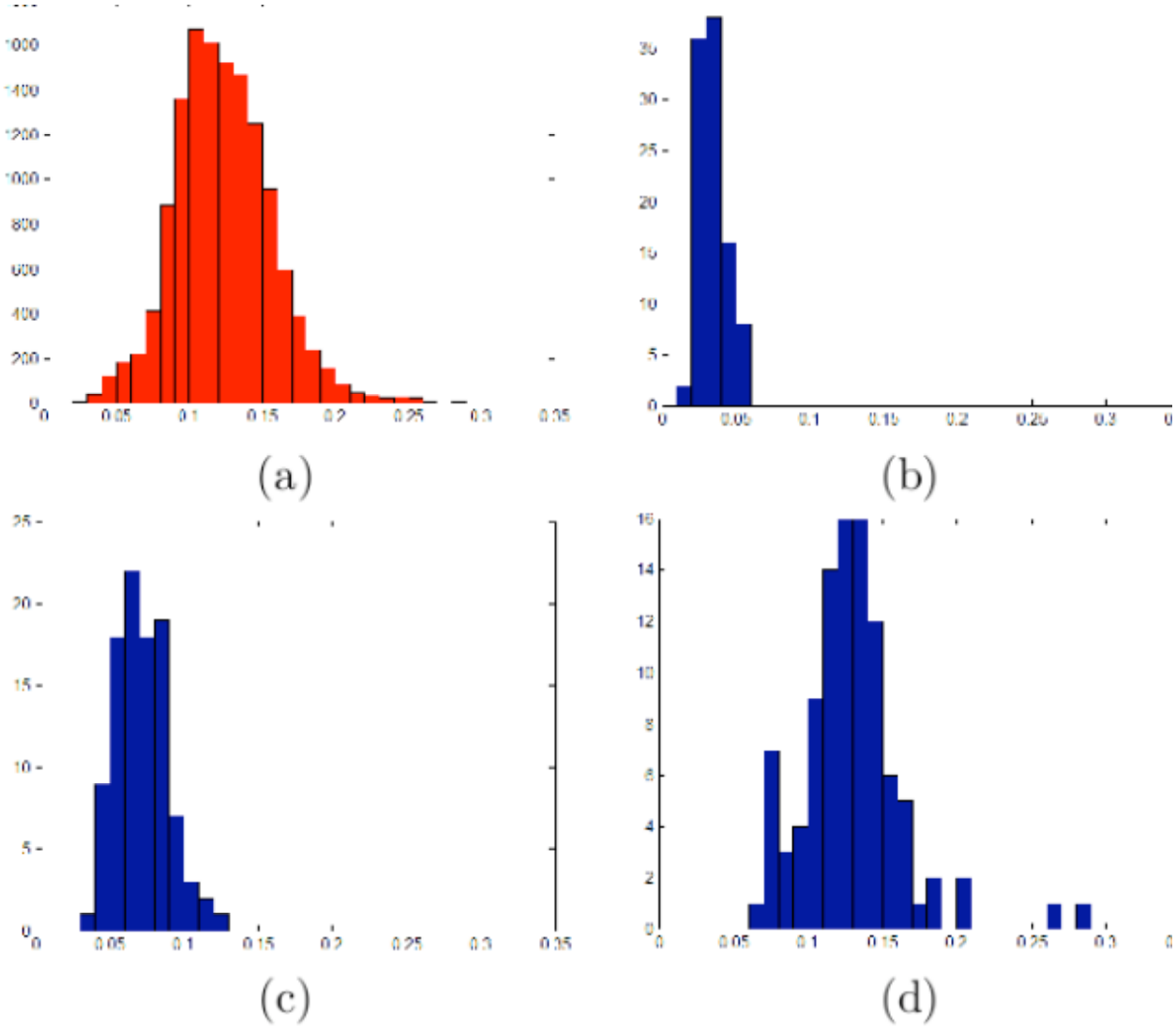

Supplementary Figure 5. Histograms Illustrating Landmark Propagation (**a**) histogram illustrating the distribution of the (approximate) cP-distances on dataset A (primate molar teeth). The three groups of 100 pairs for which we show statistics are 100 pairs with minimum $\mathbf{D}_{cP}(S, S')$, 100 randomly picked pairs in the bin with $\mathbf{D}_{cP}(S, S') = 0.1$, and 100 pairs in or near the bin $\mathbf{D}_{cP}(S, S') = 0.21$. Specifically (**b**) is the histogram of distances $\mathbf{d}_P(a(L), L')$ for the 100 pairs with smallest $\mathbf{D}_{cP}(S, S')$, (**c**) is the histogram of distances $\mathbf{d}_P(a(L), L')$ for 100 randomly picked pairs with $\mathbf{D}_{cP}(S, S') \sim 0.1$, and (**d**) is the histogram of distances $\mathbf{d}_P(a(L), L')$ for the 100 pairs with $\mathbf{D}_{cP}(S, S') \sim 0.21$.

Supplementary Discussion

Successes on particularly difficult cases

Researchers lacking familiarity with the taxa comprising the datasets used may tend to assume they were chosen to augment success rates. This is absolutely not the case. Our datasets were initially chosen and collected for entirely different projects; the goal of the project for which teeth were sampled was to evaluate incremental changes in tooth form through primate phylogeny. This project is still under preparation. Therefore taxa were included regardless of apparent high degrees of similarity. Some exceptional successes by the algorithm used on this dataset are worth noting:

1. All *Adapis* specimens were successfully distinguished as such when treated as unknowns. Workers have noted the pervasive similarity between the teeth of *Adapis* and *Hapalemur griseus* (18), claiming that they may even be impossible to separate without additional anatomical information.
2. *Cantius* was successfully distinguished from *Teilhardina*. Workers have noted the pervasive geometric similarity between teeth of these two taxa as evidence of recent divergence from a common ancestor (19).
3. *Eosimias* was successfully distinguished from *Tarsius*. Workers have suggested that *Eosimias* might actually be a tarsiiform given the similarity between their teeth (20).
4. Three different species of *Galago* were correctly classified (Fig. 4). Our sample included nine galagos: four *G. demidovii* specimens, three *G. senegalensis* specimens; and two *G. alleni* specimens. Treated as unknowns, each and every specimen was assigned as a nearest neighbor to another individual in its correct species. The molar teeth of especially the first two listed species are nearly identical, with no described differences in the literature. Boyer (1) noted that *G. alleni* has lower crowned teeth, likely corresponding to its relatively more omnivorous diet, but the pattern of its cusp arrangement is still very similar to the other species. It is worth noting that OD landmarks were not as successful at this task, mis-identifying one of galago specimens as a *Loris* (see Supplementary Table 4)

Significance of classification errors in second lower molar dataset

Generally speaking, both observer determined (OD) landmarks and automatically geometrically determined (GD) alignments done by our Automated Correspondence Determination Algorithm (ACDA) were surprisingly successful at classifying to the genus level and higher, taxa that are typically recognized by many additional skeletal and soft tissue characters besides the morphology of the second mandibular molar. In many cases, there are no specifically described molar features reported to separate various genera. Upon closer inspection the mis-classifications that did occur, actually reveal more about the geometric structure of the sample, than of short-comings in either method. Some specimens were mis-classified by both the GD and OD landmarks. One such specimen, in the genus *Hapalemur* (BMNH 84.10.20), was classified as either *Microcebus* (OD) or *Nycticebus* (GD). These constitute incorrect classifications at both genus and family levels. However, this problematic *Hapalemur* specimen is in a species (*H. simus*) that actually has molars quite distinct from those of the other two *Hapalemur* specimens, which are in the species *H. griseus*. In fact, we would not haved predicted the teeth of these two *Hapalemur* species to be morphologically close to each other no matter how they were measured.

Another such example is a specimen of *Nycticebus* (AMNH 101508), which was incorrectly classified as *Arctocebus* by ODLP-distances and *Donrussellia* by the GD method. This specimen represents a different species or subspecies from other *Nycticebus* in the sample. It represents *N. coucang javanicus*. Boyer (1) noted that this subspecies was noticeably different from other subspecies in having greater occlusal relief. This morphology is apparently driving the classification differences as well, because *Arctocebus* differs from most other lorisid genera in having higher occlusal relief (1) similar to that also exhibited by *Donrussellia*. Additionally, our ACDA mis-classifies one *Arctocebus* as AMNH 101508 – reflecting the same phenomenon.

The order-level mis-classification of two specimens of fossil primates USNM 9545 (*Paromomys*) and PU 14270 (*Plesiolestes*) as basal fossil euprimates or fossil primate outgroups, respectively (by both methods) is interesting because it reflects the conclusions of students of primate evolutionary anatomy that these early diverging forms are all extremely similar to one another. This is also reflected by the OD landmarks and GD correspondences in cases where they classify specimens of *Leptacodon*, a primate outgroup member, as the primate *Purgatorius*, and vice versa. For some of these specimens, it is very possible that the anatomical geometries are almost completely overlapping, and that information on additional anatomical structures (e.g., other teeth besides molars – like incisors or premolars) is needed to separate them consistently.

Our ACDA mis-classifies a *Hapalemur griseus* specimen as *Adapis*, surely reflecting the previously noted similarity between these two taxa (18), but also reflecting the fact that there is only one other *H. griseus* specimen in our sample, making the chance of inaccurate classification due to random factors excessively high.

Two mis-classifications by our ACDA are more difficult to explain: the mis-classification of one *Arctocebus* as *Adapis* is not expected (although these taxa are generally similar in gross-morphology and dietarily significant aspects of shape). Finally, one problematic error is the mis-match of a specimen of the dermopteran *Cynocephalus* with a galago. These taxa have dramatically different teeth. Inspection of this error shows that the correspondence map chosen by the algorithm is incorrect. It matches the hypoconid of *Cynocephalus* with the entoconid of *Galago* (for instance). We see this as a minor problem specific to our particular example analysis for the following reasons: 1) it is the only instance of such a mistake in any analysis that we detected – see below. 2) There are several parameters that can be adjusted and potentially optimized for better classfication results. We have not attempted to optimize these parameters in this study in order to get a more realistic sense of what the algorithm will be capable for the average user.

Placement of *Megaladapis*

The family attribution of *Megaladapis* is considered uncertain. Originally it was considered a close relative of *Lepilemur* and part of its family (10). More recently molecular evidence has supported its position as a basal lemurid (21). *Adapis* and adapids more generally are considered by many to represent the basal stock from which extant strepsirrhine euprimates evolved (22). Furthermore, the teeth and dentition of *Adapis* in particular have been noted for their similarity to those of *Hapalemur* (18), as well as *Megaladapis* (23). Based on these observations *Adapis* or *Megaladapis*-like teeth have been hypothesized as primitive for lemuriforms (23).

Because of uncertainty about phylogenetic attribution, in our classification analyses, *Megaladapis* was only included at the ordinal level. Both ODLP and cP methods indicate an attribution to euprimates, which is correct based on other skeletal information. Additionally both

methods link it with the same specimen of *Adapis* (Qu 10966). The next four nearest neighbors as determined by GD correspondences include two specimens of *Lemur* (AMNH 100598 and AMNH 170741) and two more of *Adapis* (Q.I.71 and Qu11117) constraining the affinities of the *Megaladapis* tooth. On one hand, these linkages do not provide evidence for a close relationship to *Lepilemur*. On the other hand, they provide additional evidence that *Megaladapis*' teeth retain primitive morphology as previously suggested, and still likely represent a plausible antecedent to the tooth shape of both *Microcebus* and *Lepilemur*.

Significance of errors in first metatarsal dataset

Among all analyses on all bones, success rates were lowest for the genus level classification of this dataset. More than a reflection of improper placement of landmarks, or inaccurate correspondence mappings, this seems likely to represent a true lack of generic level differences among some of the species sampled. Looking at genus level success rates for Cercopithecidae only, neither observer nor the computer scored higher than 8 out of 12 correct classifications. That there is truly a lack of genus-level variation would not be surprising as no one has previously described generic level differences in this bone for these cercopithecids.

The taxa responsible for the remaining majority of errors exhibited by the cP classification are *Microcebus*, *Galagoides*, and *Otolemur*. *Microcebus* is not thought particularly closely related to the other two taxa [although mouse lemurs are the only lemuriforms to share detailed cranial similarities with the Galagidae (24)]; however, the fact that both observers' landmarks confuse it with *Galagoides*, like the cP correspondences, suggests that they have similar morphologies. The mixed classification of *Galagoides* as *Otolemur* and vice versa by our ACDA is perhaps not so surprising as these taxa are closely related, and except for absolute size differences, appear very similar, again with generic level differences in this element having never been previously described as separating these two taxa. The relatively high success of the two observers at differentiating the two is actually harder to explain.

Significance of errors in radius dataset

The majority of errors in this dataset are created by mis-classifications of *Pan paniscus* (Bonobo) as *Pan troglodytes* (Chimpanzee). Most likely we have given ourselves an impossible task here as these two species are very closely related and have similar behaviors. There is no biological reason why we would predict strong morphological differences between these two taxa. Otherwise, the remainder of the errors represent mis-classifications of *Pongo* and *Gorilla* as *Pan*. At the very least both ODLP and cP methods indicate the distinctness of the distal radius of *Homo sapiens*.

Discussion of the error in algorithmic approximation to the continuous Procrustes distance

In ref [35] of the main paper, it is proved, under mild technical conditions on the surfaces, that if the continuous Procrustes distance between S and S' is small, then there must be a conformal map m from S to S' for which $d(S, S'; m)$ as small as well. More precisely (see Theorem 3.10 in [35]), there exists a constant C, independent of S', such that $d(S, S'; m) \leq C D_{cP}(S, S')^{1/4}$ once $C D_{cP}(S, S')$ is sufficiently small. The constant C and the upper bound of the range $(0,\varepsilon_0)$ of values for $D_{cP}(S, S')$ that are "sufficiently small" are not quantified explicitly in ref. [35] of the paper, so that this theorem is not an immediately practical tool.

This theorem does indicate, however, that when $C D_{cP}(S, S')$ is sufficiently small, the area-preserving map a that minimizes the cP-functional $d(S, S'; a)$ can be viewed as a small

deformation of a conformal map, or, equivalently, as a map with small conformal distortion. By searching in the space of conformal maps (which is a small-dimensional space, and eminently searchable), and (heuristically constructed) nearby area-preserving maps for each, we strive to get a good estimate for the "correct" conformal m , and thus (by deforming it to be area-preserving) for the "correct" a. We do not have an estimate controlling the error made in our approximation, and we have thus no bound on how close we are to the "correct" m or a; such bounds will be for future mathematical work. On the other hand, in practice the area-preserving correspondence maps produced by our algorithm perform very well, and for the (fairly simple) surfaces we considered we expect that we truly identify m and a close to optimally.

Discussion of Landmark Propagation

Here we quantify the statement in the main paper that "Fig. 2 shows that the propagated landmarks $a(L)$ typically turn out to be very close to those of the "true" landmarks L' ". More precisely, we have run the landmark propagation on a larger number of pairs (300). To quantify the "fit" of $a(L)$ and L', we computed, for each pair of surfaces S and S', the discrete Procrustes distance[1] $\mathrm{d}_P(L', a(L))$ between the set of expert-observer-placed landmarks L' on surface S' and the set of "landmarks" $a(L)$ on S' obtained by propagating (using the computer-generated area-preserving map a) the set of expert-observer-placed landmarks L on S.

We carried out this computation for three groups of 100 pairs of surfaces, all taken from dataset A (lemur molars). More specifically, we took, for our first group of pairs, the 100 pairs in this dataset with the smallest (approximate) cP-distances; these are the cases where we have the most confidence in our algorithms, as well as in the biological relevance of the numerical value of the cP-distance. For the second group, we picked 100 pairs with cP-distance approximately 0.1, which is the mean of all the cP-distances for dataset A. For the third group we picked 100 pairs in the large cP-distance tail of the distribution. Results are shown in Supplementary Table 8 and Supplementary Figure 5.

In supplementary figure 5 we show in (a) the histogram of the entire collection of pairwise distances $\mathbf{D}_{cP}(S, S')$ for all S, S' in out tooth dataset. The histograms of root mean square deviation [the Procrustes distances $\mathrm{d}_P(L', a(L))$] between the expert-observer-placed landmarks on the surface S' and the marks on S' obtained by propagating the expert-observer-placed landmarks on S for the three groups are shown in (b), (c) and (d).

In supplementary table 8 we provide statistics for the three groups. It is interesting to note that the mean cP-distance is proportional to (and slightly larger than) the root mean square deviation of the propagated landmarks with respect to the "true" landmarks. This confirms the match between cP-distance and ODLP-distance illustrated by figure 1 in the main text.

In figure 2 of the main text, the pairs of surfaces S and S' were deliberately chosen to be not very close, so as to illustrate the propagation under non-ideal circumstances. In the left column, for example, the tooth models (from the same dataset for which the statistics were compiled) have approximate cP-distance of 0.07; the average squared norm deviation $\mathrm{d}_P(a(L), L')$ between the set of expert-landmarks on S' and those algorithmically propagated from S is also 0.07. The statistics provided here thus illustrate that the closeness between $a(L)$ and L', shown in figure 2 in the main text, is indeed fairly typical.

[1] This is also the average root-mean-square distance between the labeled points in $a(L)$ and L', i.e. $\mathrm{d}_P(a(L), L') = \left[N^{-1} \sum_{p_j \in L} \|a(p_j) - p'_j\|^2\right]^{1/2}$, where N is the total number of landmarks ($N = \#L = \#L'$), and for each j, p'_j is the landmark on $\mathcal{S}'$ corresponding to p_j on $\mathcal{S}$.

References

1. Boyer DM (2008) Relief index of second mandibular molars is a correlate of diet among prosimian primates and other euarchontan mammals. *J. Hum. Evol.* 55:1118-1137.
2. Garland M & Heckbert PS (1997) Surface simplification using quadric error metrics. *SIGGRAPH '97: Proceedings of the 24th annual conference on Computer graphics and interactive techniques* (ACM Press/Addison-Wesley Publishing Co.), pp 209–216.
3. Desbrun M, Meyer M, Schroder P, & Barr AH (1999) Implicit fairing of irregular meshes using diffusion and curvature flow. *SIGGRAPH '99: Proceedings of the 26th annual conference on Computer graphics and interactive techniques* (ACM Press/Addison-Wesley Publishing Co.), pp 317–324.
4. Taubin G (2000) Geometric signal processing on polygonal meshes. *Eurographics'2000 - State of The Art Report*.
5. Cope ED (1883) Note on the trituberculate type of superior molar and the origin of the quadrituberculate. *Am. Nat.* 17:407-408.
6. Osborn HF (1907) *Evolution of Mammalian Molar Teeth: To and From the Tritubercular Type* (The Macmillan Company, New York) p 250.
7. Gregory WK (1934) A half century of Trituberculy, the Cope-Osborn theory of dental evolution with a revised summary of molar evolution from fish to man. *Proc. Am.Phil. Soc.* 73:169-317.
8. Simpson GG (1936) Studies of the earliest mammalian dentitions. *Dental Cosmos* 78:791-800 and 940-953.
9. Szalay FS & Delson E (1979) *Evolutionary History of the Primates* (Academic Press, San Diego) p 580.
10. Schwartz JH & Tattersall I (1985) *Evolutionary Relationships of living lemurs and lorises (Mammalia, Primates) and their potential affinities with European Eocene Adapidae* (American Museum of Natural History, New York) p 100.
11. Richmond BG & Strait DS (2000) Evidence that humans evolved from a knuckle-walking ancestor. *Nature* 404:382-384.
12. Szalay FS & Dagosto M (1988) Evolution of Hallucial Grasping in the Primates. *J. Hum. Evol.* 17(1-2):1-33.
13. Mitteroecker P & Gunz P (2009) Advances in Geometric Morphometrics. *Evol. Bio.* 36:235-247.
14. Wiley DF*, et al.* (2005) Evolutionary Morphing. *Proc. IEEE Vis. 2005*:8.
15. Mantel N (1967) The detection of disease clustering and a generalized regression approach. *Cancer Res.* 27:209-220.
16. Bunn JM*, et al.* (2011) Dirichlet normal surface energy of tooth crowns, a new technique of molar shape quantification for dietary inference, compared with previous methods in isolation and in combination. *Am. J. Phys. Anthropol.* in press.
17. Boyer DM, Evans AR, & Jernvall J (2010) Evidence of dietary differentiation among late Paleocene-early Eocene plesiadapids (Mammalia, Primates). *Am. j. Phys. Anthropol.* 142:194-210.
18. Gingerich PD (1975) Dentition of Adapis parisiensis and the evolution of Lemuriform primates. *Lemur Biology,*, ed Tattersall I (Plenum Press, , New York.), p 65.
19. Gingerich PD, Franzen JL, Habersetzer J, Hurum JH, & Smith BH (2010) *Darwinius masillae* is a Haplorhine - Reply to Williams et al. (2010). *J. Hum. Evol.* 59:574-579.

20. Simons EL (2003) The Fossil Record of Tarsier Evolution. *Tarsiers: past, present, and future*, eds Wright PC, Simons EL, & Gursky S.
21. Orlando L*, et al.* (2008) DNA from extinct giant lemurs links archaeolemurids to extant indriids. *BMC Evol. Bio.* 8(121):doi:10.1186/1471-2148-1188-1121
22. Seiffert ER, Perry JMG, Simons EL, & Boyer DM (2009) Convergent evolution of anthropoid-like adaptations in Eocene adapiform primates. *Nature* 461:1118-1121.
23. Seligsohn D (1977) Analysis of species-specific molar adaptations in strepsirhine primates. *Contrib. Primatol.* 11:1-116.
24. MacPhee RDE (1981) Auditory regions of primates and eutherian insectivores, morphology, ontogeny, and character analysis. *Contrib. Primatol.* 18:1-282.